Ferroelectric switching dynamics in $0.5Ba(Zr_{0.2}Ti_{0.8})O_3$-$0.5(Ba_{0.7}Ca_{0.3})TiO_3$ thin films

J. P. B. Silva,[1,2,a] K. Kamakshi,[3,a] R. F. Negrea,[4] C. Ghica,[4] J. Wang,[5] G. Koster,[5] G. Rijnders,[5] F. Figueiras,[2,6] M. Pereira,[1] and M. J. M. Gomes[1]
[1]*Centre of Physics, University of Minho, Campus de Gualtar, 4710-057 Braga, Portugal*
[2]*IFIMUP and IN-Institute of Nanoscience and Nanotechnology, Departamento de Física e Astronomia, Faculdade de Ciências da Universidade do Porto, Rua do Campo Alegre 687, 4169-007 Porto, Portugal*
[3]*Department of Physics, Madanapalle Institute of Technology & Science, Madanapalle 517325, Andhra Pradesh, India*
[4]*National Institute of Materials Physics, 105 bis Atomistilor, 077125 Magurele, Romania*
[5]*Faculty of Science and Technology and MESA$^+$ Institute for Nanotechnology, Inorganic Materials Science, University of Twente, P. O. Box 217, 7500 AE Enschede, The Netherlands*
[6]*Department of Physics and CICECO-AIM, University of Aveiro, 3810-193 Aveiro, Portugal*

(Received 14 June 2018; accepted 4 August 2018; published online 21 August 2018)

In this work, the ferroelectric characteristics of $0.5Ba(Zr_{0.2}Ti_{0.8})O_3$-$0.5(Ba_{0.7}Ca_{0.3})TiO_3$ (BCZT) thin films grown on 0.7 wt. % Nb-doped (*001*)-$SrTiO_3$ (Nb:STO) single-crystal have been investigated. High-resolution transmission electron microscopy and electron energy loss spectroscopy revealed a very sharp Nb:STO/BCZT interface, while selected area electron diffraction revealed the epitaxial growth of the BCZT layer on the Nb:STO substrate. The ferroelectric nature of the BCZT films have been investigated by piezoresponse force microscopy and hysteresis loops. The effect of electric field on polarization switching kinetics has been investigated and has been analyzed by the nucleation limited switching model with a Lorentzian distribution function. The local field variation was found to decrease with the increase in the electric field, and thus, the switching process becomes faster. The peak value of the polarization current and the logarithmic characteristic switching time exhibited an exponential dependence on the inverse of electric field. This model gave an excellent agreement with the experimental polarization reversal transients throughout the whole time range. *Published by AIP Publishing*. https://doi.org/10.1063/1.5044623

Ferroelectric thin films have been investigated intensively in recent years, due to their high polarizability, which can contribute to improve the performance and efficiency of non-volatile memory devices and solar cells.[1–4]

The understanding of the polarization switching mechanism in ferroelectric films is important from the scientific point of view as well as for its applications. Various theoretical models have been developed to explain the switching kinetics in ferroelectrics.[5–7] The Kolmogorov–Avrami–Ishibashi (KAI) model describes the polarization reversal behavior of many single crystals but is not adequate for thin films.[8] Therefore, Tagantsev *et al.* proposed the nucleation limited switching (NLS) model as an alternative approach to KAI model to explain the polarization reversal kinetics.[9] This model is based on the statistics of nucleation and growth of the reversed domains.

It is known that there is an urgent demand for a material capable of replacing $Pb(Zr,Ti)O_3$ (PZT) in a broad range of applications.[10] Recently, the lead-free ferroelectric $0.5Ba(Zr_{0.2}Ti_{0.8})O_3$-$0.5(Ba_{0.7}Ca_{0.3})TiO_3$ (BCZT) ceramic has been considered as a potential candidate for various applications due to their exceptional properties.[11,12] However, these properties in thin films are still far from the exceptional values exhibited by the bulk.[13,14] Moreover, there are still no comprehensive studies on the polarization switching dynamics of BCZT thin films.

Therefore, in the present letter, the ferroelectricity in the BCZT films at the nano and macroscale level was investigated using piezoresponse force microscopy (PFM) and ferroelectric hysteresis loops (P-E), respectively. Furthermore, the polarization reversal characteristics of epitaxial BCZT thin films have been analyzed using Lorentzian distribution function for characteristic times of domain growth based on the NLS model.

A BCZT target prepared by conventional solid state reaction, as described by Silva *et al.*,[15] was used for the deposition of the corresponding thin films. BCZT thin films, with 160 nm thickness, were grown on 0.7 wt. % Nb-doped TiO_2 terminated (*001*) $SrTiO_3$ (Nb:STO) single-crystal substrates using pulsed laser deposition (PLD) as described in Silva *et al.*[16] Cross-section transmission electron microscopy (TEM) specimens have been prepared as described in Silva *et al.*[16] The transmission electron microscopy (TEM) and Scanning transmission electron microscopy (STEM) investigations have been performed on a Cs probe-corrected JEM ARM 200F analytical electron microscope equipped with a Gatan Quantum SE Image Filter for Electron Energy Loss Spectroscopy (EELS) and EELS—Spectrum Image (EELS—SI) analysis in the STEM mode. Imaging and spectral data processing have been made using specialized routines under Gatan Digital Micrograph. Piezoresponse force microscopy (PFM) was carried out using a scanning probe microscope (NT-MDT Ntegra Aura) equipped with internal lock-in amplifiers. A commercial NT-MDT doped silicon probes with Pt coating with a radius of curvature of about

[a]Authors to whom correspondence should be addressed: josesilva@fisica.uminho.pt and kamakshikoppole@gmail.com

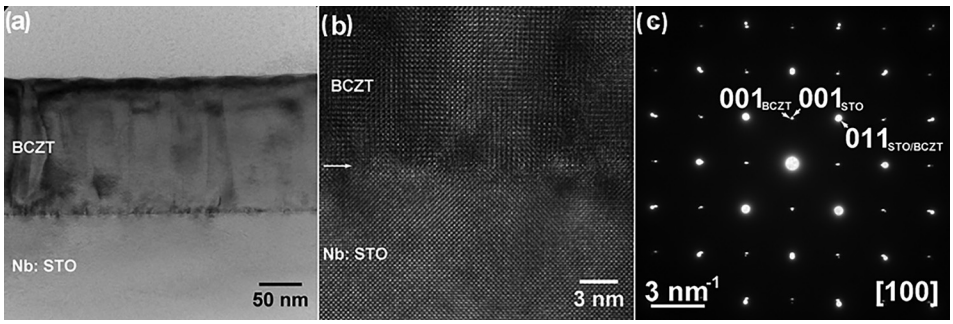

FIG. 1. (a) TEM image at low-magnification showing BCZT/Nb: STO structure; (b) HRTEM image of BCZT-Nb: STO interface; and (c) SAED pattern corresponding to TEM image.

20 nm, resonance frequency of ∼130 kHz, and spring constant k of about 3 N/m have been used in PFM. The topographic, the piezo-response amplitude, and the phase images were edited via a *WSxM 5.0 develop 8.0* software. All piezoresponse force microscopy and spectroscopy studies were done out-of-resonance (10–30 kHz) in order to decrease electrostatic responses with the correspondent topographic cross-talk. For the macroscopic ferroelectric measurements, gold (Au) top circular electrodes, with a diameter of 1 mm each, were grown by thermal evaporation using metal shadow mask patterning. The ferroelectric hysteresis loops (P-E) were measured, by investigating the capacitors of Nb:STO/BCZT/Au, with a modified Sawyer-Tower circuit using a sinusoidal signal at a frequency of 1 kHz. The polarization switching transients have been studied by applying a bipolar square pulse with different amplitudes. Experimental method for transient current measurements is Sawyer-Tower circuit. In this, a 50 Ω resistor is connected in series with Nb:STO/BCZT/Au device and the input bipolar square pulse signal is applied across them. The voltage drop across the resistor is measured by cathode-ray oscilloscope (CRO) in the x-t mode.[17]

The structural quality of the BCZT thin film deposited on the Nb:STO substrate has been investigated by TEM. Figure 1(a) shows a low-magnification TEM image of the Nb:STO/BCZT structure. The 160-nm thick BCZT layer has a compact and continuous epitaxial structure with a low roughness. The HRTEM image shown in Fig. 1(b) evidences the high crystallinity of the BCZT thin film and very sharp Nb:STO/BCZT interface. Moreover, the selected area electron diffraction (SAED) pattern in Fig. 1(c) reveals the epitaxial growth of the BCZT layer on the Nb:STO substrate. The crystallographic relation between the substrate and BCZT thin film is $[001]_{\text{Nb: STO}}||[001]_{\text{BCZT}}$.

Figure 2 shows the high angle annular dark field—scanning transmission electron microscopy (HAADF-STEM) image at low-magnification of the Nb:STO/BCZT structure and the EELS-SI maps (on the right side of Fig. 2) revealing the distribution of O, Ca, Ti, Sr, Zr, and Ba elements inside the green rectangle from HAADF-STEM image. The RGB (Red-Green-Blue) image (down-right) was obtained overlapping the Ba M and Sr L maps and clearly point to a very sharp interface without any perceptible atomic interdiffusion, therefore confirming the high quality of these BCZT thin films deposited on the Nb:STO substrate.

Figure 3 shows a topographic scan of the BCZT thin film taken by AFM revealing a uniform and dense microstructure with an average roughness of ≈0.1 nm and with no evidence of cracking or defects.

The ferroelectricity at the nanoscale level was investigated by PFM. Simultaneous recording of piezoresponse amplitude and phase scans [Figures 3(b) and 3(c)] enables a visualization of the spatial correlation between strong contrast regions suggesting ferroelectric domains with 200–300 nm size. The hysteretic dependencies of the amplitude and phase piezo-signals to the applied bias electric field are shown in Fig. 3(d) and clearly reveal the local switching of a ferroelectric domain in the BCZT thin film.[18] The piezo-response phase signal exhibits a well-shaped hysteresis loop with the ≈180° phase reversing. The asymmetric shape of the hysteresis loops is due to the difference in work functions between the bottom (Nb:STO) and top (Pt) electrodes.[19,20] The saturation is reached above 5 Vdc, and the local coercive voltages (V_c) are taken as the minima of amplitude loop[20] and are found to be approximately −0.9 and +1.8 V. The coercive field (E_c) was estimated by using the relation $V_c = E_c.t$,[21] where t is the thickness of the BCZT film and was estimated to be ≈81 kV cm^{-1}.

Figure 4(a) exhibits the room temperature electric field dependent polarization-electric field (P–E) hysteresis loops of the BCZT film. The hysteresis loops reveal that as the voltage increases, the P–E loop saturates. As the electric field increased from 60 kV cm^{-1} to 150 kV cm^{-1}, both saturation polarization (P_s) and the remnant polarization (P_r) increases. The average P_s and P_r values are shown in Table I for the different applied electric fields. For an electric field of 150 kV cm^{-1}, a well-saturated hysteresis loops was obtained with a P_s of 30.3 μC cm^{-2} and a P_r of 21.3 μC cm^{-2}. The obtained values for P_r and P_s are higher than those reported in the literature for epitaxial BCZT thin films.[22,23] Moreover, the coercive field of 60 kV cm^{-1} is much higher than the

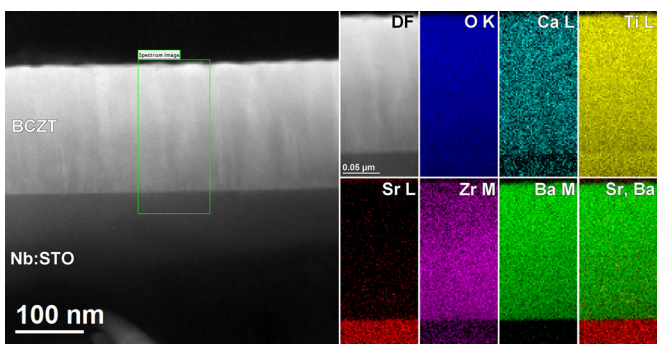

FIG. 2. HAADF-STEM image at a low-magnification of BCZT/Nb: STO structure and EELS-SI maps showing the elemental distribution inside of a green rectangle. RGB map (down-right) was obtained overlapping the Ba M and Sr L maps.

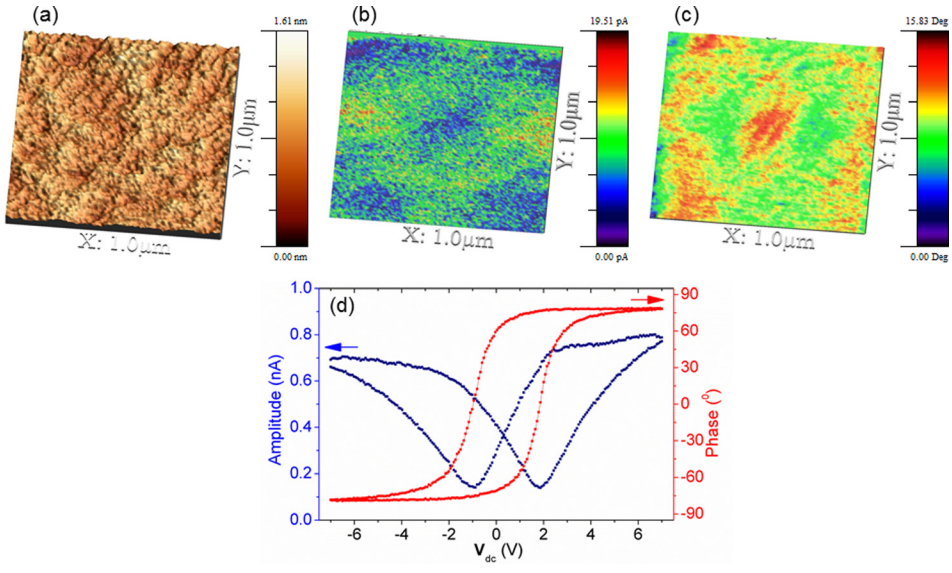

FIG. 3. (a) Topography, (b) off-plane piezo-response amplitude, and (c) phase scans. (d) Local PFM amplitude butterfly loops and phase hysteresis loops of the BCZT thin film.

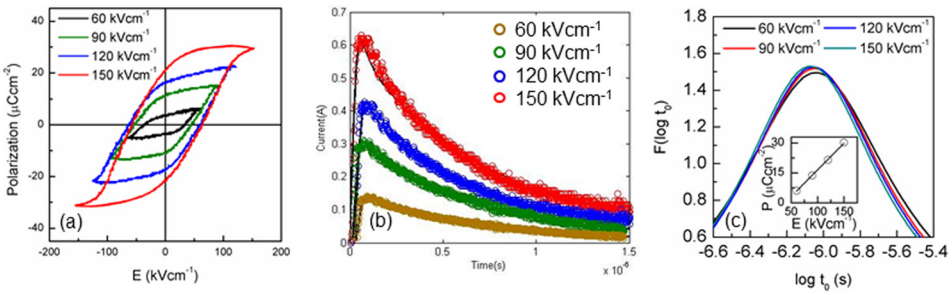

FIG. 4. (a) Electric field dependent P–E loops of the BCZT film, (b) polarization reversal transients of BCZT films at different electric fields (discrete points correspond to experimental data and solid line corresponds NLS theory), and (c) Lorentzian distribution function and inset shows variation of P_s with the electric field.

TABLE I. The effect of the applied electric field on the average remnant and spontaneous polarization (P_r and P_s) and on the switching parameters for the BCZT thin film.

Electric field (kV cm^{-1})	Pr (μC cm^{-2}) (P-E loops)	Ps (μC cm^{-2}) (P-E loops)	Ps (μC cm^{-2}) (switching)	i_m (mA)	t_m (s)
60	3.7	5.5	6.1	133	1.1×10^{-7}
90	11.1	14.0	13.7	293	9.9×10^{-8}
120	17.0	22.0	21.5	419	7.6×10^{-8}
150	21.3	30.3	30.2	612	5.7×10^{-8}

value of 1.75 kV cm^{-1} for the bulk BCZT ceramic, which is a consequence of much smaller grains in comparison with the bulk ceramic.[20] However, the measured coercive field is similar to the one observed in other BCZT films deposited in STO substrates.[22] In addition, the difference between the coercive fields obtained from the P-E loops and from the PFM measurements can be related to the different top electrical boundary conditions (PFM uses a silicon probe with Pt coating, while P-E loop measurements uses Au electrodes).[24]

The understanding of process of polarization reversal is one of the important characteristics of ferroelectric materials due to its direct relevance in memory applications. The ferroelectric polarization reversal behavior of BCZT films was studied using the square pulse at different pulse amplitudes. The discrete points in Fig. 4(b) correspond to the experimentally observed values of temporal dependence of switching current for BCZT films at different electric fields in range of 60–150 kV cm^{-1}. The polarization reversal phenomenon arises due to the nucleation of new domains, their propagation, and coalescence. The peak value of current (i_m) occurs at a time (t_m), and their variation with pulse amplitudes is shown in Table I. The i_m values show an exponential dependence of reversal electrical field as per Merz's law,[25] and the activation field was found to be 64 kV cm^{-1}. The t_m value was found to be 5.7×10^{-8} s at a field of 150 kV cm^{-1}, which is faster when compared to other ferroelectric thin films.[8,26,27] As shown in Table I, as the electric field increases 2.5 times, the i_m increases 4.6 times, while the t_m decreases 2 times. This could be explained by the contribution of new switched regions. The spontaneous polarization (P_s) was estimated by calculating the area under the switching current transients (Q) using the relation $Q = 2P_s A$, where "A" is the area of the electrode.[28] The P_s values estimated from the polarization reversal are in good agreement with those of values obtained from the P-E loop, as shown in Table I.

Kolmogorov-Avrami-Ishibashi proposed first a theoretical model known as KAI model to explain the ferroelectric switching kinetics in single crystals based on classical theory of statistical nucleation and unrestricted domain growth. Later, Tagantsev *et al.*[9] proposed the nucleation limited switching (NLS) model based on statistics of nucleation and domain growth rate, and this model has been chosen to analyze the switching kinetics of present BCZT thin films. The NLS model assumes that the sample is as ensemble of regions in which switching takes place independently and simultaneously and thus each region may have different switching characteristic time t_o. It represents the characteristic time for

domain growth and is proportional to average distance between the nuclei, divided by the domain wall speed. Since each region have different t_o values, NLS model assumed a broad distribution of characteristic switching time t_o and is represented by F(log t_o). The temporal dependence of polarization current has been expressed by considering the Lorentzian distribution function of logarithmic switching times in the definite regions of the film as follows:[8]

$$i(t) = 2P_sA\frac{d}{dt}\left\{\int_{-\infty}^{\infty}\left[1-\exp\left(-\frac{t}{t_0}\right)^n\right]F(\log t_0)d(\log t_0)\right\}, \tag{1}$$

where $F(\log t_o)$ is the distribution function for $\log t_o$ as follows:[8]

$$F(\log t_0) = \frac{K}{\pi}\left(\frac{\omega}{(\log t_0 - \log t_1)^2 + \omega^2}\right), \tag{2}$$

where K is a normalized constant, ω is the half-width at half maximum, and t_1 peak time value of Lorentz distribution function. In general, either Gaussian or Lorentz distribution function can be used in statistically independent random process like switching kinetics, film growth models, etc. However, Vleck has shown the dipolar broadening of magnetic resonance lines in crystals with randomly distributed dipole impurities obey to Lorentzian distribution.[29] Theoretical studies also revealed that the distribution of any interaction field component in the system of dilute aligned dipoles obeys to Lorentzian distribution.[30] Moreover, it is known that ferroelectric thin films contain dipole defects which hinder the domain wall motion. Therefore, a Lorentz distribution function is considered in the NLS model.

Equation (1) was used to fit the experimental data of polarization reversal curves and the corresponding fitted curves were shown by solid lines in Fig. 4(b). The corresponding logarithmic distribution function of Eq. (2) is shown in Fig. 4(c). The excellent agreement of NLS curves with the experimental data in whole time region suggest that films consist of different regions in which the polarization reversal take place independently. The existence of independent regions is also corroborated from the linear field dependence of P_s in the studied electric field range, as shown in the inset of Fig. 4(c). Therefore, the new switching regions are contributing to the polarization as electric field increases.

The values of parameters t_1 and ω are obtained from the fittings and then are related to microscopic parameters using the approximations[8,31]

$$\log t_1 \approx \frac{\propto_{dm}}{E}, \tag{3}$$

$$\omega \approx \frac{\Gamma \propto_{dm}}{E^2}, \tag{4}$$

where $\propto_{dm}$ is the activation field for domain wall motion and Γ is the full width at half maximum in the Lorentzian local field distribution function. F($\bar{E}$) is related to the concentration of pinning sites and is described as follows:[8,31]

$$F(\bar{E}) = \frac{K}{\pi}\left(\frac{\Gamma}{\bar{E}^2 + \Gamma^2}\right), \tag{5}$$

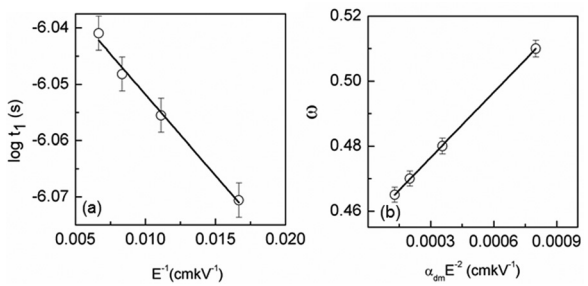

FIG. 5. (a) Plot of log t_1 versus 1/E and (b) plot of w versus $\frac{\propto_{dm}}{E^2}$.

where $\bar{E}$ is the local electric field distribution that exists at pinning sites. The presence of non-homogenous structural defects, such as domain walls, dislocations, or grain boundaries, acts as pinning sites of polarization reversal and causes local field vacations between the switching and non-switching regions.[32] Figures 5(a) and 5(b) show the plot of log t_1 as a function of E^{-1} and the plot of w versus $\frac{\propto_{dm}}{E^2}$, respectively.

The values of $\propto_{dm}$ and Γ are found to be 3 and 62 kV cm^{-1}, respectively. This activation energy of Γ can be related to the threshold energy for the pinned domains and is in good agreement with values obtained from Merz's law. This activation field is higher than the one observed in $BaTiO_3$ crystals, but lower than the ones reported for PZT, $BiFeO_3$, and $Ba_{0.8}Sr_{0.2}TiO_3$ thin films.[25,27,33–35]

In summary, high structural quality epitaxial BCZT thin films were grown by pulsed laser deposition on single crystalline Nb:STO (*001*) substrates. The ferroelectric nature of films was examined at the nanoscale level by PFM and at the macroscopic level by P-E hysteresis loops. The BCZT films exhibit promising ferroelectric properties with a notable remnant polarization of 21.3 μC cm^{-2} and a coercive field of 60 kV cm^{-1}. The domain growth limited switching process based on NLS model is found to be appropriate to describe the reversal kinetics and the logarithmic characteristic switching time obeyed the Lorentzian distribution. Moreover, the values of P_s from the switching and P-E loops are in good agreement. The peak values of polarization current and logarithmic characteristics switching time obey the exponential dependence on the electric field. The t_m values are found to be faster as compared to previous reports. Therefore, this work provides a comprehensive study about the polarization reversal behavior on BCZT thin films with enhanced ferroelectric properties.

This work was supported by (i) Portuguese Foundation for Science and Technology (FCT) in the framework of the Strategic Funding No. UID/FIS/04650/2013 and (ii) Project Norte-070124-FEDER-000070 Nanomateriais Multifuncionais. Part of this work was supported by the COST Action MP1308 "Towards Oxide-Based Electronics (TO-BE)." The authors acknowledge the CERIC-ERIC Consortium for access to experimental facilities and financial support under Proposal No. 20157018. The authors J.P.B.S. and F.F. are grateful for financial support through the FCT Grant Nos. SFRH/BPD/92896/2013 and SFRH/BPD/80663/2011, respectively. R.F.N. and C.G. acknowledge the financial support from the Romanian Ministry of Research and Innovation in the frame of the Core Program No. PN18-110101. The authors would also

like to acknowledge P. B. Tavares, Centro de Química da Universidade de Trás-os-Montes e Alto Douro, for the supply of the 0.5BZT-0.5BCT PLD target.

[1]A. Ghosh, G. Koster, and G. Rijnders, APL Mater. **4**, 066103 (2016).
[2]D.-F. Pan, G.-F. Bi, G.-Y. Chen, H. Zhang, J.-M. Liu, G.-H. Wang, and J.-G. Wan, Sci. Rep. **6**, 22948 (2016).
[3]J. P. B. Silva, F. L. Faita, K. Kamakshi, K. C. Sekhar, J. A. Moreira, A. Almeida, M. Pereira, A. A. Pasa, and M. J. M. Gomes, Sci. Rep. **7**, 46350 (2017).
[4]H. Matsuo, Y. Noguchi, and M. Miyayama, Nat. Commun. **8**, 207 (2017).
[5]A. Ghosh, G. Koster, and G. Rijnders, Adv. Funct. Mater. **26**, 5748 (2016).
[6]Y.-H. Shin, I. Grinberg, I.-W. Chen, and A. M. Rappe, Nature **449**, 881 (2007).
[7]A. Gruverman, "Polarization behavior in thin film ferroelectric capacitors at the nanoscale," in *Scanning Probe Microscopy of Functional Materials*, edited by S. Kalinin and A. Gruverman (Springer, New York, NY, 2010).
[8]K. C. Sekhar and R. Nath, Appl. Phys. Lett. **94**, 102905 (2009).
[9]A. K. Tagantsev, I. Stolichnov, N. Setter, J. S. Cross, and M. Tsukada, Phys. Rev. B **66**, 214109 (2002).
[10]J. Rödel, K. G. Webber, R. Dittmer, W. Jo, M. Kimura, and D. Damjanovic, J. Eur. Ceram. Soc. **35**, 1659 (2015).
[11]W. Liu and X. Ren, Phys. Rev. Lett. **103**, 257602 (2009).
[12]J. Gao, D. Xue, Y. Wang, D. Wang, L. Zhang, H. Wu, S. Guo, H. Bao, C. Zhou, W. Liu, S. Hou, G. Xiao, and X. Ren, Appl. Phys. Lett. **99**, 092901 (2011).
[13]M. Acosta, N. Novak, V. Rojas, S. Patel, R. Vaish, J. Koruza, G. A. Rossetti, and J. Rödel, Appl. Phys. Rev. **4**, 041305 (2017).
[14]J. P. B. Silva, K. Kamakshi, K. C. Sekhar, E. C. Queirós, J. A. Moreira, A. Almeida, M. Pereira, P. B. Tavares, and M. J. M. Gomes, J. Phys. D: Appl. Phys. **49**, 335301 (2016).
[15]J. P. B. Silva, E. C. Queirós, P. B. Tavares, K. C. Sekhar, K. Kamakshi, J. A. Moreira, A. Almeida, M. Pereira, and M. J. M. Gomes, J. Electroceram. **35**, 135 (2015).
[16]J. P. B. Silva, J. Wang, G. Koster, G. Rijnders, R. F. Negrea, C. Ghica, K. C. Sekhar, J. A. Moreira, and M. J. M. Gomes, ACS Appl. Mater. Interfaces **10**, 15240 (2018).
[17]I. K. Yoo, "Testing and characterization of ferroelectric thin film capacitors," in *Nanoscale Phenomena in Ferroelectric Thin Films*, edited by S. Hong (Kluwer Academic, Boston, 2004).
[18]Q. R. Lin, D. Y. Wang, B. C. Luo, R. Ding, D. L. Lorenzen, and S. Li, Appl. Surf. Sci. **331**, 477 (2015).
[19]A. Jalalian, A. M. Grishin, X. L. Wang, Z. X. Cheng, and S. X. Dou, Appl. Phys. Lett. **104**, 103112 (2014).
[20]V. S. Puli, D. K. Pradhan, S. Adireddy, R. Martínez, P. Silwal, J. F. Scott, C. V. Ramana, D. B. Chrisey, and R. S. Katiyar, J. Phys. D: Appl. Phys. **48**, 355502 (2015).
[21]S. M. Neumayer, I. N. Ivanov, M. Manzo, A. L. Kholkin, K. Gallo, and B. J. Rodriguez, J. Appl. Phys. **118**, 224101 (2015).
[22]B. C. Luo, D. Y. Wang, M. M. Duan, and S. Li, Appl. Phys. Lett. **103**, 122903 (2013).
[23]M.-J. Choi, J.-R. Lim, J.-S. Choi, J.-H. Eom, B.-J. Park, K.-S. Kim, D. Kim, and S.-G. Yoon, Scr. Mater. **108**, 96 (2015).
[24]S. V. Kalinin, B. J. Rodriguez, S. Jesse, Y. H. Chu, T. Zhao, R. Ramesh, S. Choudhury, L. Q. Chen, E. A. Eliseev, and A. N. Morozovska, Proc. Natl. Acad. Sci. U. S. A. **104**, 20204 (2007).
[25]J. Y. Jo, H. S. Han, J.-G. Yoon, T. K. Song, S.-H. Kim, and T. W. Noh, Phys. Rev. Lett. **99**, 267602 (2007).
[26]O. Lohse, M. Grossmann, U. Boettger, D. Bolten, and R. Waser, J. Appl. Phys. **89**, 2332 (2001).
[27]D. Pantel, Y.-H. Chu, L. W. Martin, R. Ramesh, D. Hesse, and M. Alexe, J. Appl. Phys. **107**, 084111 (2010).
[28]N. Dabra, J. S. Hundal, A. Nautiyal, K. C. Sekhar, and R. Nath, J. Appl. Phys. **108**, 024108 (2010).
[29]J. H. V. Vleck, Phys. Rev. **74**, 1168 (1948).
[30]J. R. Klauder and P. W. Anderson, Phys. Rev. **125**, 912 (1962).
[31]J. P. B. Silva, K. C. Sekhar, S. A. S. Rodrigues, A. Khodorov, J. Martín-Sanchez, M. Pereira, and M. J. M. Gomes, Curr. Appl. Phys. **12**, 1144 (2012).
[32]W. Li and M. Alexe, Appl. Phys. Lett. **91**, 262903 (2007).
[33]H. H. Wieder, J. Appl. Phys. **28**, 367 (1957).
[34]J. F. Scott, L. Kammerdiner, M. Parris, S. Traynor, V. Ottenbacher, A. Shawabkeh, and W. F. Oliver, J. Appl. Phys. **64**, 787 (1988).
[35]J. P. B. Silva, K. C. Sekhar, A. Almeida, J. Agostinho Moreira, J. Martín-Sánchez, M. Pereira, A. Khodorov, and M. J. M. Gomes, J. Appl. Phys. **112**, 044105 (2012).